Thin liquid films with time-dependent chemical reactions sheared by an ambient gas flow

Achim Bender,* Peter Stephan, and Tatiana Gambaryan-Roisman
Institute for Technical Thermodynamics, Technische Universität Darmstadt, 64287 Darmstadt, Germany
(Received 29 December 2016; published 3 August 2017)

Chemical reactions in thin liquid films are found in many industrial applications, e.g., in combustion chambers of internal combustion engines where a fuel film can develop on pistons or cylinder walls. The reactions within the film and the turbulent outer gas flow influence film stability and lead to film breakup, which in turn can lead to deposit formation. In this work we examine the evolution and stability of a thin liquid film in the presence of a first-order chemical reaction and under the influence of a turbulent gas flow. Long-wave theory with a double perturbation analysis is used to reduce the complexity of the problem and obtain an evolution equation for the film thickness. The chemical reaction is assumed to be slow compared to film evolution and the amount of reactant in the film is limited, which means that the reaction rate decreases with time as the reactant is consumed. A linear stability analysis is performed to identify the influence of reaction parameters, material properties, and environmental conditions on the film stability limits. Results indicate that exothermic reactions have a stabilizing effect whereas endothermic reactions destabilize the film and can lead to rupture. It is shown that an initially unstable film can become stable with time as the reaction rate decreases. The shearing of the film by the external gas flow leads to the appearance of traveling waves. The shear stress magnitude has a nonmonotonic influence on film stability.

DOI: 10.1103/PhysRevFluids.2.084002

I. INTRODUCTION

Fuels and engine oils form wall films in combustion chambers of internal combustion engines after injection through droplet-wall interactions and develop deposits on ports, cylinder walls, and pistons [1–3]. Typically, the turbulent gas flow inside the combustion chamber shears and spreads the film. Deposits form from these liquid films through cross-linking and chemical reactions [4–7]. These deposits have a negative influence on the combustion cycle [8] and lead to decreased engine efficiency and an increased amount of pollutants.

Under engine operating conditions higher wall temperatures lead to an increase in deposit formation [9]. The wall temperature typically increases in the region of film rupture and formation of dry spots. It can be suggested that deposits tend to be formed during dewetting preferably near the three-phase contact line, where the liquid-gas interface meets the wall. This preferential deposition formation near the contact line has been observed for several multicomponent systems, in particular, in urea-water solutions [10]. The observed behavior makes it important to understand the processes that lead to film instability and breakup under combustion chamber conditions.

Even though the stability of thin liquid films has been studied in a wide variety of scenarios, the effect of chemical reactions in the film has not received much attention. Dagan and Pismen [11] investigated the impact of a multistable kinetic system on the solutal Marangoni effect. von Gottberg [12] conducted a linear stability analysis for a rapid, reversible interfacial reaction acting in two semi-infinite liquid phases. Qi and Johnson [13] studied a falling reactive film with viscosity being a function of composition. Braun *et al.* [14] examined the influence of temperature-dependent surface tension on a drop spreading on a solid plate in the presence of an isothermal chemical reaction.

*bender@ttd.tu-darmstadt.de

Gallez *et al.* [15] investigated the influence of a surface chemical reaction on the dynamics of a thin liquid film on a solid substrate. The chemical reaction leads to surface tension gradients and gives rise to dynamics that cannot be found in the pure hydrodynamic model of the free surface.

Trevelyan *et al.* [16] considered a vertical falling film in contact with a wall of constant temperature. A first-order chemical reaction is present in the film. The liquid-gas interface is adiabatic and of constant reactant concentration. This leads to an unlimited supply of reactant in the film through diffusive mass transport. A stationary distribution of reactant concentration is established in the film after an initial transient phase. That investigation aims to find the film behavior when a small deviation from the stationary state occurs. The chemical reaction is considered to be slow, leading to small Damköhler numbers. A double perturbation analysis is conducted to find the evolution equation for the film height. Analysis of the basic state reveals that a slow exothermic chemical reaction has a stabilizing effect on the film as long as the surface tension decreases with increasing temperature. Additionally, an exothermic reaction reduces mass transport. An endothermic reaction, however, has a destabilizing effect on the film and may lead to film rupture.

Trevelyan and Kalliadasis [17] extended the work of Trevelyan *et al.* [16] to large Péclet numbers and included higher orders in the derivation of the evolution equation in order to cover the whole feedback cycle of the problem. The chemical reaction alters the surface tension through temperature gradients, which affects the film evolution, which in turn affects the rate of reaction and therefore the reactive energy release.

Matar and Spelt [18] investigated a thin liquid film that is bounded on both sides by an inviscid fluid with constant density and temperature. An exothermal chemical reaction is present in the film following an Arrhenius law. Gravitational effects are not considered since the film is so thin that the Bond number is very low. The van der Waals forces play a role for the film thickness considered in that work. The energy release from the reaction decreases the film density and viscosity and may lead to thermocapillary effects. Density and viscosity are a function of temperature and composition. Density reduction has a stabilizing effect, while the viscosity reduction and thermocapillary effect are destabilizing.

Peirera *et al.* [19] investigated a horizontal film with a reactive surface active agent (surfactant). The reacting surfactant has a destabilizing effect on the film and gives rise to solitary pulses at the interface.

In the present work we examine a thin liquid film that is sheared by a turbulent gas flow and heated from below by a wall with constant temperature. A first-order chemical reaction is present in the film and the amount of reactant in the film is limited. The heat released (for an exothermic reaction) or consumed (for an endothermic reaction) by the reaction leads to temperature gradients at the liquid-gas interface and gives rise to the Marangoni effect. Long-wave theory [20,21] is used to reduce the complexity of the problem and obtain an evolution equation for the film thickness. In contrast to most previous investigations, we consider a time-dependent chemical reaction where the reaction rate slows down as more and more reactant is consumed. Additionally, the influence of shear stress at the interface on stability and evolution is included.

The rest of this paper is structured as follows. The problem is formulated, the relevant governing equations are given, and the first-order evolution equation for the film height is derived in Sec. II. In Sec. III the linear stability of the problem is examined, followed by some remarks on the numerical scheme in Sec. IV. Results are presented in Sec. V, where a discussion of the results is given as well. A summary is given in Sec. VI.

II. FORMULATION

A. Problem definition

A thin two-dimensional film on a rigid, planar, and impermeable wall with constant temperature T_w (Fig. 1) is considered. The film is thin enough that buoyancy can be neglected but so thick that van der Waals forces do not a play role. The ambient gas flow shears the film at the liquid-gas

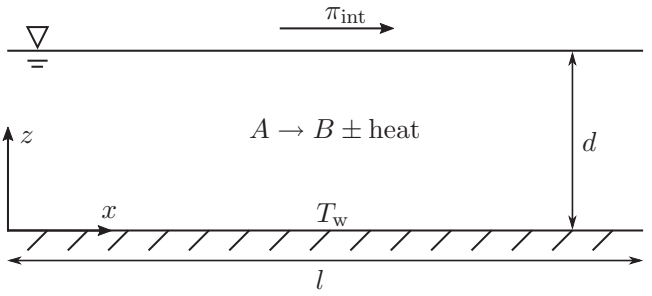

FIG. 1. Sketch of the two-dimensional problem. The thin film rests on a wall with constant temperature and is sheared by a gas flow. A chemical reaction takes place in the film.

interface with a constant shear stress π_{int}, which accounts for the effect of the outer gas flow. The film consists of two species (named arbitrarily A and B). Initially the film consists only of species A. There is no mass flux through the liquid-gas interface, so the sum of the mass of the two species within the film remains constant. There is a first-order chemical reaction going on in the film, where

$$A \rightarrow B \pm \text{heat}. \tag{1}$$

Species A as the reactant undergoes a first-order (endothermic or exothermic) chemical decays while it reacts with the product species B. With increasing time the concentration of A will decrease, while the concentration of B will increase, leading to a reduced reaction rate. Both species are assumed to be passive, meaning that the concentration profile has no effect on the flow field. Furthermore, the fluid is assumed to be nonvolatile, so evaporation can be neglected. The heat generated or consumed by the reaction leads to temperature gradients at the liquid-gas interface and gives rise to a thermocapillary Marangoni effect, which in turn affects the fluid flow, interface shape, and shear rate at the interface. However, the temperature differences are small enough that material values can be calculated for an average temperature without considerable error. The Marangoni effect induced by a concentration gradient is not taken into account. The liquid-gas interface is further assumed to be adiabatic because the thermal conductivity in the gas is much smaller than in the liquid phase.

B. Derivation of the evolution equation

The governing equation for mass, momentum, energy, and species transport of the reactant for a two-dimensional film have the following dimensional form:

$$u_x + w_z = 0, \tag{2}$$

$$u_t + uu_x + wu_z = -\frac{1}{\rho} p_x + \nu(u_{xx} + u_{zz}), \tag{3}$$

$$w_t + uw_x + ww_z = -\frac{1}{\rho} p_z + \nu(w_{xx} + w_{zz}) - g, \tag{4}$$

$$T_t + uT_x + wT_z = a(T_{xx} + T_{zz}) + r\frac{qc}{\rho c_p}, \tag{5}$$

$$c_t + uc_x + wc_z = D(c_{xx} + c_{zz}) - rc. \tag{6}$$

Here u and w are the velocity components in the x (parallel to the wall) and z (perpendicular to the wall) directions, T is the temperature, p is the pressure, c is the concentration of the reactant species A, g is the gravitational acceleration, and t is the time. The material values ρ, ν, c_p, a, and D of the liquid phase are the fluid density, kinematic viscosity, heat capacity, thermal conductivity, and binary diffusion coefficient, respectively. The heat released or consumed by the reaction q does

not depend on the temperature. For an endothermic reaction this parameter takes negative values ($q < 0$) and for an exothermic reaction positive values ($q > 0$). The reaction rate r is a function of temperature $r = r(T)$ and follows an Arrhenius equation for a first-order reaction

$$r = r_0 e^{-E_A/RT}, \tag{7}$$

where r_0 is the preexponential factor, E_A is the activation energy, and R the ideal gas constant.

The boundary conditions on the bottom wall $z = 0$ correspond to no-slip and no-penetration conditions, constant wall temperature, and no species flux and are given by

$$u = 0, \quad w = 0, \quad T = T_w, \quad c_z = 0. \tag{8}$$

At the liquid-gas interface $z = h$ we formulate the normal and tangential stress balance including surface tension effects and the shear stress from the outer gas

$$\begin{aligned} \underline{\underline{T}} \cdot \underline{n} \cdot \underline{n} &= -p + 2\mu \frac{u_x\left(h_x^2 - 1\right) - h_x(u_z + w_x)}{\left(1 + h_x^2\right)} \\ &= \sigma \frac{h_{xx}}{\left(1 + h_x^2\right)^{3/2}}, \end{aligned} \tag{9}$$

$$\begin{aligned} \underline{\underline{T}} \cdot \underline{n} \cdot \underline{\tau} &= \mu \frac{\left(1 - h_x^2\right)(u_z + w_x) + 2h_x(w_z - u_x)}{\left(1 + h_x^2\right)^{1/2}} \\ &= \frac{\partial \sigma}{\partial T}(T_x + h_x T_z) + \pi_{\text{int}}. \end{aligned} \tag{10}$$

Furthermore, there is no heat transfer from or to the outer gas and no species transport across the interface

$$T_x h_x + T_z = 0, \tag{11}$$

$$c_x h_x + c_z = 0. \tag{12}$$

Finally, the kinematic boundary condition at the interface must be fulfilled:

$$h_t + u h_x - w = 0. \tag{13}$$

In Eqs. (9) and (10) $\underline{\underline{T}}$ is the stress tensor, which, using the Stokes hypothesis and the assumption of an incompressible Newtonian fluid, can be expressed as

$$\underline{\underline{T}} = -p\underline{\underline{I}} + \mu[\nabla \underline{u} + (\nabla \underline{u})^T], \tag{14}$$

with the identity tensor $\underline{\underline{I}}$, the velocity vector $\underline{u} = [u, w]$, and the dynamic viscosity μ. The normal $\underline{n}$ and tangential $\underline{\tau}$ vectors can be expressed as

$$\underline{n} = \frac{h_x \underline{e_x} + \underline{e_z}}{\left(1 + h_x^2\right)^{1/2}}, \quad \underline{\tau} = \frac{\underline{e_x} + h_x \underline{e_z}}{\left(1 + h_x^2\right)^{1/2}}. \tag{15}$$

The surface tension of a pure liquid decreases with increasing temperature and vanishes at the critical point. It is assumed that species concentration gradients do not influence the surface tension and that the surface tension is only a function of temperature ($\partial\sigma/\partial T = d\sigma/dT$). Moreover, a linear dependence of the surface tension on temperature is assumed [22]

$$\sigma = \sigma_0 + \frac{d\sigma}{dT}(T - T_0), \tag{16}$$

with $d\sigma/dT = \text{const}$ and the surface tension σ_0 at reference temperature T_0. For typical liquids $d\sigma/dT < 0$ can be observed. The Marangoni effect is modeled assuming that temperature gradients at the interface will lead to a tangential stress (10).

The balance equations and boundary conditions can be nondimensionalized. The time is nondimensionalized with the reaction time scale, while velocities are nondimensionalized with respect to the velocity of the outer gas flow. Accordingly, the nondimensional parameters read

$$\epsilon = \frac{d}{l}, \quad X = \frac{x}{l} = \frac{x\epsilon}{d}, \quad Z = \frac{z}{d}, \quad U = \frac{\mu u}{\pi_{\text{int}} d}, \quad W = \frac{\mu w}{\pi_{\text{int}} d\epsilon},$$
$$\tau = r_0 e^{-\beta} t, \quad \Theta = \frac{T - T_{\text{w}}}{\frac{|q|c_0}{\rho c_p}}, \quad P = \frac{p}{\pi_{\text{int}}}, \quad C = \frac{c}{c_0}, \quad H = \frac{h}{d},$$

where d is the initial film thickness, l is the film length, which is also a length scale of film deformation, and c_0 is the initial concentration of species A in the film.

Note that the term $qc_0/\rho c_p$ in the definition of Θ constitutes a characteristic temperature difference. This can be understood as the temperature change in a film established after the reaction is finished completely in the absence of heat transport.

Additionally, the Damköhler number Da, the dimensionless interfacial shear stress Π, the Prandtl number Pr, the Schmidt number Sc, the nondimensional gravity G, the surface tension force S, the Marangoni number Ma, and the dimensionless activation energy β are defined as important nondimensional parameters of the problem:

$$\text{Da} = \frac{d^2 r_0 e^{-\beta}}{\nu}, \quad \Pi = \frac{d^2 \pi_{\text{int}}}{\mu\nu}, \quad \text{Pr} = \frac{\nu}{a}, \quad \text{Sc} = \frac{\nu}{D}, \quad G = \frac{d^3 g}{\nu^2},$$
$$S = \frac{\sigma d}{\mu\nu}, \quad \text{Ma} = -\frac{d\sigma}{dT}\frac{d\frac{qc_0}{\rho c_p}}{\mu a}, \quad \beta = \frac{E_{\text{A}}}{RT_{\text{w}}}.$$

The Damköhler number Da describes the ratio between the viscosity time scale and the reactive time scale. The dimensionless interfacial shear stress Π compares the interfacial shear stress to viscous stresses in the film. The Prandtl number Pr is defined as the ratio between viscous momentum transfer and conductive heat transfer, while the Schmidt number Sc describes the ratio between viscous momentum transfer and diffusive mass transfer. Gravity and surface tension are made nondimensional by comparing the gravitational force to viscous forces and the stresses arising from surface tension to viscous stresses, respectively. The Marangoni number Ma is defined using the characteristic temperature difference $qc_0/\rho c_p$ described above. The activation energy is made nondimensional with the ideal gas constant and the wall temperature.

The dimensionless variables are now plugged back into the governing equations (2)–(6) and boundary conditions (8)–(13). This yields, for the nondimensional governing equations,

$$U_X + W_Z = 0, \tag{17}$$
$$\text{Da}\, U_\tau + \epsilon\Pi(UU_X + WU_Z) = -\epsilon P_X + \epsilon^2 U_{XX} + U_{ZZ}, \tag{18}$$
$$\text{Da}\,\epsilon W_\tau + \epsilon^2\Pi(UW_X + WW_Z) = -P_Z + \epsilon^3 W_{XX} + \epsilon W_{ZZ} - \frac{G}{\Pi}, \tag{19}$$
$$\text{Da}\,\text{Pr}\,\Theta_\tau + \epsilon\,\text{Pr}\,\Pi(U\Theta_X + W\Theta_Z) = \epsilon^2\Theta_{XX} + \Theta_{ZZ} + \text{sgn}(q)\text{Da}\,\text{Pr}\,Ce^{\beta\Theta/(\Theta+1)}, \tag{20}$$
$$\text{Da}\,\text{Sc}\,C_\tau + \epsilon\,\text{Sc}\,\Pi(UC_X + WC_Z) = \epsilon^2 C_{XX} + C_{ZZ} - \text{Da}\,\text{Sc}\,Ce^{\beta\Theta/(\Theta+1)}. \tag{21}$$

For the lower boundary at $Z = 0$ the boundary conditions are

$$U = 0, \quad W = 0, \quad \Theta = 0, \quad C_Z = 0. \tag{22}$$

While the boundary conditions for the liquid-gas interface at $Z = H$ are

$$-P + 2\epsilon \frac{U_X\left(\epsilon^2 H_X^2 - 1\right) - H_X(U_Z + \epsilon^2 W_X)}{1 + \epsilon^2 H_X^2} = \epsilon^2 \frac{S}{\Pi} \frac{H_{XX}}{\left(1 + \epsilon^2 H_X^2\right)^{3/2}}, \tag{23}$$

$$\frac{\left(1 - \epsilon^2 H_X^2\right)(U_Z + \epsilon^2 W_X) + 2\epsilon^2 H_X(W_Z - U_X)}{\left(1 + \epsilon^2 H_X^2\right)^{1/2}} = -\epsilon \frac{\mathrm{sgn}(q)\mathrm{Ma}}{Pr\,\Pi}(\Theta_X + H_X\Theta_Z) + 1, \tag{24}$$

$$\Theta_Z + \epsilon^2 H_X \Theta_X = 0, \tag{25}$$

$$C_Z + \epsilon^2 H_X C_X = 0, \tag{26}$$

$$H_\tau + \frac{\Pi\epsilon}{\mathrm{Da}}(U H_X - W) = 0. \tag{27}$$

For the following derivation rapid mass diffusion in the Z direction is assumed ($C_{ZZ} = 0$), leading to a constant concentration over the film height (well mixed). This assumption is valid for thin films [23,24].

A double perturbation analysis [16] is carried out in ϵ and Da to derive an evolution equation for the film height. The basic assumption is that the film is thin in comparison with the length scale of the film thickness variation. It is assumed that the scale of the film thickness variation is the film length, so $\epsilon \ll 1$. Further, the chemical reaction is slow ($\mathrm{Da} \ll 1$), but $\epsilon < \mathrm{Da} \ll \epsilon^{1/2}$. Using these relations, all dependent variables can be expanded as shown for the dimensionless temperature

$$\Theta \propto \Theta^{00} + \mathrm{Da}\,\Theta^{01} + \epsilon\Theta^{10} + \mathrm{Da}^2\Theta^{02} + \epsilon\mathrm{Da}\,\Theta^{11} + \epsilon^2\Theta^{20} + O(\mathrm{Da}^3). \tag{28}$$

Strong surface tension effects $S = O(\epsilon^{-2})$ are assumed so that the surface tension term enters the equation in the zeroth order $O(0)$. The tangential shear stress, originating from Marangoni forces, can be found in $O(\epsilon)$. Thus, it is required that $\epsilon\,\mathrm{sgn}(q)\mathrm{Ma}\,\Theta_X/\mathrm{Pr}\,\Pi = O(\epsilon)$, with $\Theta_X = O(\mathrm{Da})$ and $\mathrm{Pr} = (1)$ leading to $\mathrm{Ma} = O(\mathrm{Da}^{-1})$. Finally, $G = O(1)$ and $\Pi = O(1)$ are assumed, so gravitation and the shear stress influence from the outer gas enter the velocity field in zeroth order and $\mathrm{Sc} = O(1)$. For convenience, the substitutions $\tilde{S} = \epsilon^2 S$ and $\widetilde{\mathrm{Ma}} = \mathrm{Da}\,\mathrm{Ma}$ are made. Plugging the results of the $O(0)$, $O(\mathrm{Da})$, and $O(\epsilon)$ analysis in the kinematic boundary condition (13) leads to an order ϵ equation for the evolution of the dimensionless film height H,

$$H_\tau + \frac{\epsilon}{\mathrm{Da}}\left\{\frac{1}{2}\Pi H^2 + \epsilon\left[\frac{1}{3}H^3(\tilde{S}H_{XXX} - GH_X) - \frac{1}{2}\widetilde{\mathrm{Ma}}H_X H^3 e^{-\tau}\right]\right\}_X = 0. \tag{29}$$

The second term of the evolution equation can be identified as the influence of the shear stress from the outer gas flow. The third term includes surface tension effects that act to minimize the interfacial energy. The fourth term arises through gravity. The last term finally originates from surface tension gradients at the free surface. These surface tension gradients result from temperature gradients that are developed due to the heat release or consumption during the chemical reaction. Notice the exponential decay of this term with time ($e^{-\tau}$). In the chosen setting with limited reactant supply the reaction rate decreases exponentially with τ and the effect of the reaction on the interface temperature decreases accordingly.

III. LINEAR STABILITY ANALYSIS

The evolution equation (29) is linearized around the undisturbed state to examine the stability of the basic state. The dimensionless film height H can be written as

$$H(x,\tau) = 1 + \delta H'(x,\tau), \tag{30}$$

with

$$\delta \ll 1. \tag{31}$$

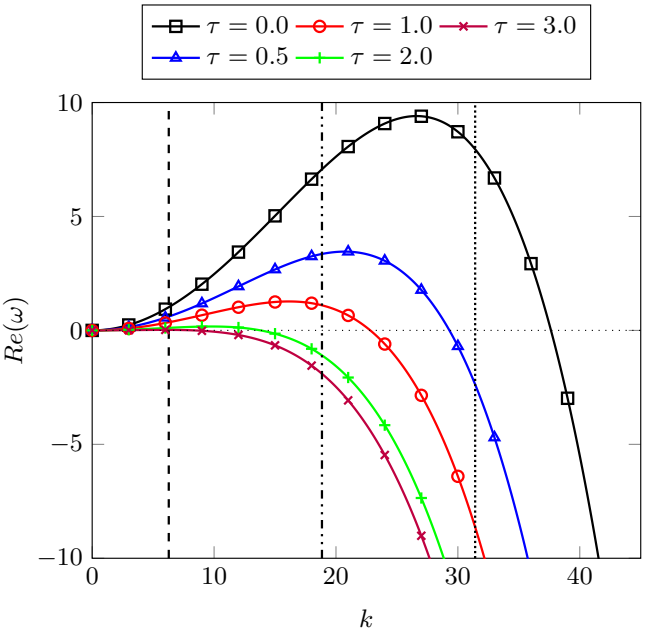

FIG. 2. Time development of the disturbance growth rate over wave number with three exemplary wave numbers highlighted for Fig. 9 (2π, 6π, and 10π).

Equation (30) is substituted into the evolution equation (29). Since δ is small, only linear terms of δ are considered. This leads to

$$H'_\tau + \frac{\epsilon}{\mathrm{Da}}\left\{\Pi H'_X + \epsilon\left[\frac{1}{3}(\tilde{S}H'_{XXXX} - GH'_{XX}) - \frac{1}{2}\widetilde{\mathrm{Ma}}\, e^{-\tau} H'_{XX}\right]\right\} = 0. \tag{32}$$

Thus, a linear equation has been derived. However, this linear equation does not have constant coefficients because of the term containing $e^{-\tau}$. If the reaction time scale is assumed to be much larger than the time scale of the growth of disturbance, we can assume $e^{-\tau} \approx$ const for the scope of this analysis, since the change in $e^{-\tau}$ is smaller than the change in τ for large times. For small times this analysis is applicable if we assume large perturbation growth rates ω (compare Fig. 2, where for $\tau = 0$, for example, the approximation is valid for $10 < k < 35$). This has already been done implicitly by choosing $\mathrm{Da} \ll 1$ in the derivation of the evolution equation. The evolution equation and this analysis is suitable for slow chemical reactions as found in many industrial applications. Under this assumption, the solutions of Eq. (32) can be sought using the normal mode approach

$$H'(x,\tau) \propto e^{\omega\tau + ikX}. \tag{33}$$

In this equation k is the wave number and ω is the growth rate of the perturbations. This ansatz is now used to derive an equation for the disturbance growth rate as a function of the wave number. The perturbations decay if the real part of the growth rate is smaller than zero $\mathrm{Re}(\omega) < 0$. The disturbance growth rate is obtained as

$$\omega = \frac{\epsilon}{\mathrm{Da}}\left\{-i\Pi k + k^2\left[\frac{\epsilon}{3}(-G - k^2\tilde{S}) - \frac{1}{2}\epsilon\,\widetilde{\mathrm{Ma}}\, e^{-\tau}\right]\right\}. \tag{34}$$

This analysis is strictly justified for fast growth of the disturbance in comparison to reaction time, which leads to $\omega \gg 1$ as the validity condition for Eq. (34). This means that this analysis is valid far from the neutral stability region.

Surface tension has a stabilizing effect. This term depends on k^4 and is consequently highly wave-number dependent. If terms of order k^2 are investigated we find a stabilizing effect as long as

$$\frac{G}{3} + \frac{1}{2}\widetilde{\mathrm{Ma}}\, e^{-\tau} > 0. \tag{35}$$

This dependence is examined further in the following. In the absence of gravitational forces ($G = 0$) every endothermic reaction ($\widetilde{\mathrm{Ma}} < 0$) leads to an unstable behavior, while an exothermic reaction leads to a stable behavior. Gravity ($G > 0$) has a stabilizing effect on the film as long as the gravity vector points from the interface to the wall. In this case endothermic reactions are stable if

$$G > \tfrac{3}{2}|\widetilde{\mathrm{Ma}}|e^{-\tau}. \tag{36}$$

Since this relation is time dependent, one may find a primarily unstable film becoming stable with time as τ increases under the assumption that the initial disturbance did not grow essentially and the linear approximation of the evolution equation stays valid. If the stabilizing effect of surface tension is negligible ($\tilde{S} = 0$), the disturbance would grow while τ satisfies the condition

$$\ln\left(\frac{3|\widetilde{\mathrm{Ma}}|}{2G}\right) > \tau. \tag{37}$$

When τ passes this point the disturbances will decay, leading to a flat film. This behavior does not depend on the film height.

Moreover, a critical wave number can be identified for which a maximum growth rate ω can be found. This wave number k_{crit} fulfills the condition

$$\frac{\partial\, \mathrm{Re}(\omega)}{\partial k} = 0, \tag{38}$$

which leads to

$$k_{\mathrm{crit}} = \sqrt{\frac{3\,\widetilde{\mathrm{Ma}} + 2G}{-4\tilde{S}}}. \tag{39}$$

The influence of the interfacial shear stress can be examined using Eq. (34). The term containing the shear stress is imaginary, so the applied interfacial shear stress does not affect the linear stability and is not expected to influence the development of the film height in the linear approximation. However, beyond the linear behavior, the interfacial shear stress affects the film stability and evolution, which will be analyzed in Sec. V.

A plot of the real part of the disturbance growth rate over wave number is shown in Fig. 2 for an endothermic reaction. One can see that the growth rate is zero for a wave number of zero. With increasing wave number the growth rate increases until it reaches a maximum value. For high wave numbers the growth rate becomes negative. Additionally, a big impact of time on the shape of the function is found. The maximum growth rate decreases with increasing time because the reaction rate decreases. The maximum growth rate also shifts to lower wave numbers with increasing time. The cutoff wave number [corresponding to the condition $\mathrm{Re}(\omega) = 0$] also decreases with increasing time. For very large times, when the reaction is completed, the linear stability is determined by the stabilizing influence of gravity and surface tension, so the disturbance growth rate is negative for all wave numbers. The influence of the initial disturbance on the development of the film height is investigated in more detail in Sec. V.

IV. NUMERICAL SCHEME

The evolution equation is a fourth-order partial differential equation. This equation is solved numerically using finite-difference discretization for the spatial derivatives. Second-order central differences are used, which require up to four neighboring points for the fourth derivative in X [25].

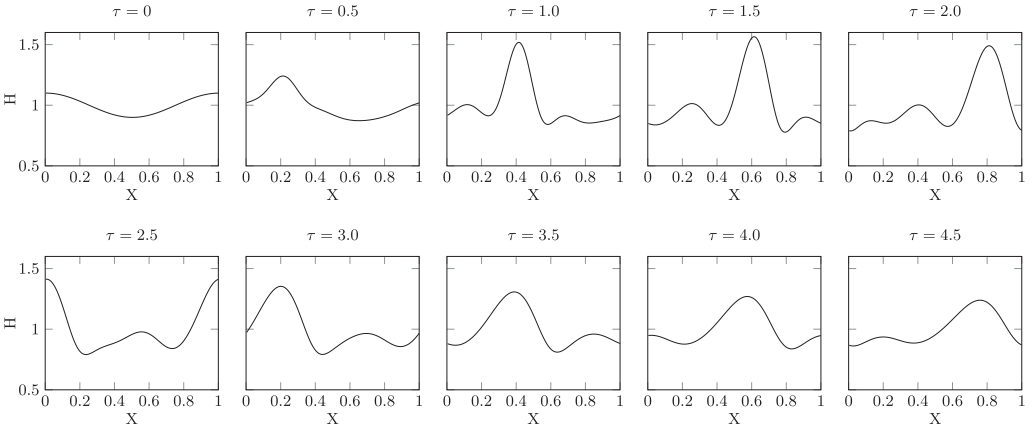

FIG. 3. Film evolution for a film with a moderate endothermic reaction.

A second-order-accurate Crank-Nicolson method is used for time. However, because of the exponential dependence of the last term in Eq. (29) on time, this scheme is not fully implicit. Therefore, rather small time steps have to be chosen to achieve convergence. Additionally, the nonlinearity of Eq. (29) makes the solution of the equation system very costly in terms of computational time. Hence, the Crank-Nicolson method is used in linearized form. The film height at time $n+1$ is equal to the film height at time n plus the difference $\tilde{h}$ at every point i:

$$H_i^{n+1} = H_i^n + \tilde{h}_i. \tag{40}$$

If the chosen time steps are small enough, it can be assumed that $\tilde{\mathbf{h}} \ll \mathbf{H} \approx 1$, where $\tilde{\mathbf{h}}$ and $\mathbf{H}$ are vectors containing the values $\tilde{h}_i$ and H_i^n for all points i, respectively. Now Eq. (40) is substituted into the discretized evolution equation. All terms containing $\tilde{\mathbf{h}}$ of higher order [$O(\tilde{\mathbf{h}})$ and $O(\tilde{\mathbf{h}}^2)$] are small compared to terms of order one and can be neglected. Using this, all terms of the evolution equation can be transformed to linear terms. Since the right-hand side of the evolution equation is equal to zero, it is now possible to formulate a system of linear equations in the form

$$\mathbf{R} \cdot \tilde{\mathbf{h}} = \mathbf{RM}, \tag{41}$$

with $\tilde{\mathbf{h}}$ as the desired solution vector. Matrix $\mathbf{R}$ collects all terms containing $\tilde{\mathbf{h}}$ or its derivatives, while matrix $\mathbf{RM}$ contains all terms independent of $\tilde{\mathbf{h}}$. This system of equations is solved for every time step using MATLAB. Periodic boundary conditions are chosen at the left and right edges of the domain to simulate an infinite film. A spatial resolution of $N_X = 300$ is found to be sufficient to describe the film shape and to compute the fourth spatial derivative with sufficient accuracy even for highly disturbed films. A time-step size of $\Delta\tau = 10^{-6}$–10^{-4} is chosen to accurately capture the film dynamics and the exponential decay of the reaction rate with time. The calculation is stopped if the film height at any point is lower than 0.001, with the assumption of film rupture occurring at that moment.

V. RESULTS

The physical parameters chosen for this section are those of a film of engine oil with a film thickness of $h = 50\ \mu$m and length $l = 1$ mm on a wall with the constant temperature $T_w = 450$ K. The chemical reaction resembles a hydrocarbon oxidation and leads to a characteristic temperature difference of $|q|c_0/\rho c_p = 60$ K (with $q = -9.2 \times 10^7\ \mathrm{J\,m^{-3}}$, $c_0 = 1$, $c_p = 1800\ \mathrm{J\,kg^{-1}\,K^{-1}}$, and $\rho = 850\ \mathrm{kg\,m^{-3}}$). This leads to the following nondimensional parameters: $\epsilon = 0.05$, $\mathrm{Da} = 0.1$, $\Pi = 0.75$, $\mathrm{Pr} = 30$, $G = 2.3 \times 10^{-3}$, $\tilde{S} = 2.2 \times 10^{-3}$, and $\widetilde{\mathrm{Ma}} = -2.3$.

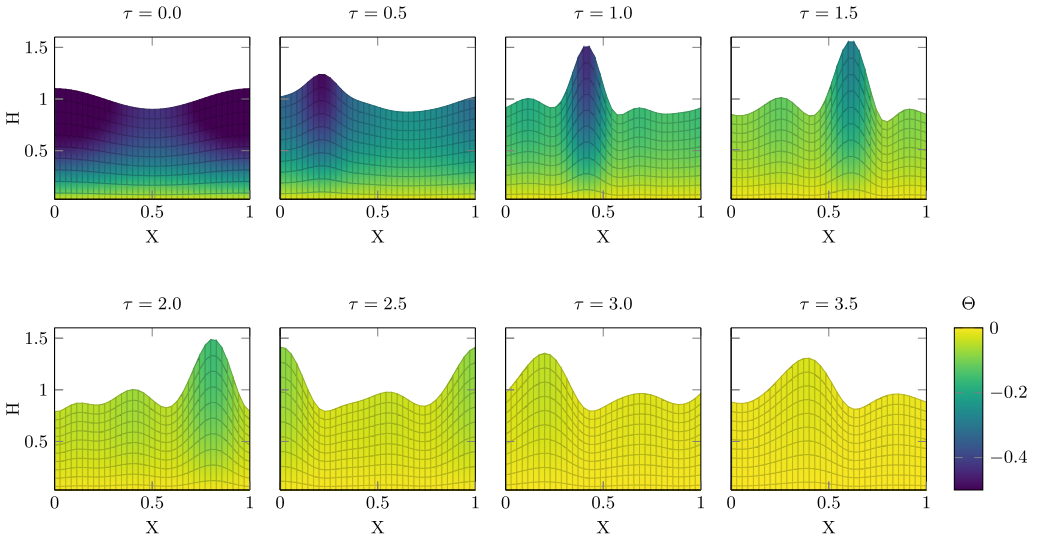

FIG. 4. Time evolution of the temperature field.

The film evolution for an exemplary moderate endothermic reaction is shown in Fig. 3. A sinusoidal initial disturbance is prescribed. The wave travels through the domain from left to right, driven by the imposed shear stress. An increase of the crest of the film can be observed for small times, leading to a maximum at $\tau \approx 1.5$, before the peak height decays again.

This interesting behavior can be explained by the influence of the Marangoni effect caused by the chemical reaction. The reaction rate has a maximum value for $\tau = 0$ and decays exponentially with time. The heat consumed by the reaction leads to the temperature profile displayed in Fig. 4. The interface temperature has a minimum value at the film crests and higher values at the wave troughs. Since surface tension decreases with temperature, the resulting surface tension field drives fluid from the troughs to the crests, leading to an increase of the peak height. As the reaction rate slows down with increasing time, less and less heat is consumed. In addition, thermal conduction reduces the temperature gradients at the film surface and thus the driving force of the instability. Surface tension and gravity are now dominant and begin leveling out the film, eventually leading to complete film flattening.

Moreover, the development of smaller side maxima around the peak can be observed, which eventually merge with the highest peak (see Fig. 3). The merging process is caused by the fact that the horizontal velocity increases with increasing film height, which is evident from Fig. 5. The horizontal velocity is zero at the wall due to the no-slip boundary condition and grows with wall distance. The velocity has its maximum on the upstream side of the highest peak, which leads to an increase of peak height and a decrease of peak width with increasing time. Consequently, the highest peak travels with a higher velocity than a smaller side peak. In Fig. 3 one can see that the highest peak has merged with a downstream side peak at $\tau = 2.0$. The side peaks on the upstream side of the highest peak travel with a lower velocity and can be observed for a longer time. Eventually though, only one film height maximum remains and the film returns to an almost sinusoidal shape.

The observed behavior is exemplary for a certain set of parameters. In the following a parametric study of the influence of interfacial shear stress, surface tension, gravity, reaction parameters, and wavelength of the initial disturbance on film evolution is presented. The evolution of the maximum film height is chosen as an indicator for the behavior of the entire film. Here $\Pi_0 = 0.75$, $\tilde{S}_0 = 2.2 \times 10^{-3}$, $G_0 = 2.3 \times 10^{-3}$, and $\widetilde{\mathrm{Ma}}_0 = -2.3$ are defined as standard parameters for a thin engine oil film ($d = 50\ \mu$m) sheared by an ambient flow at inner engine conditions and with a

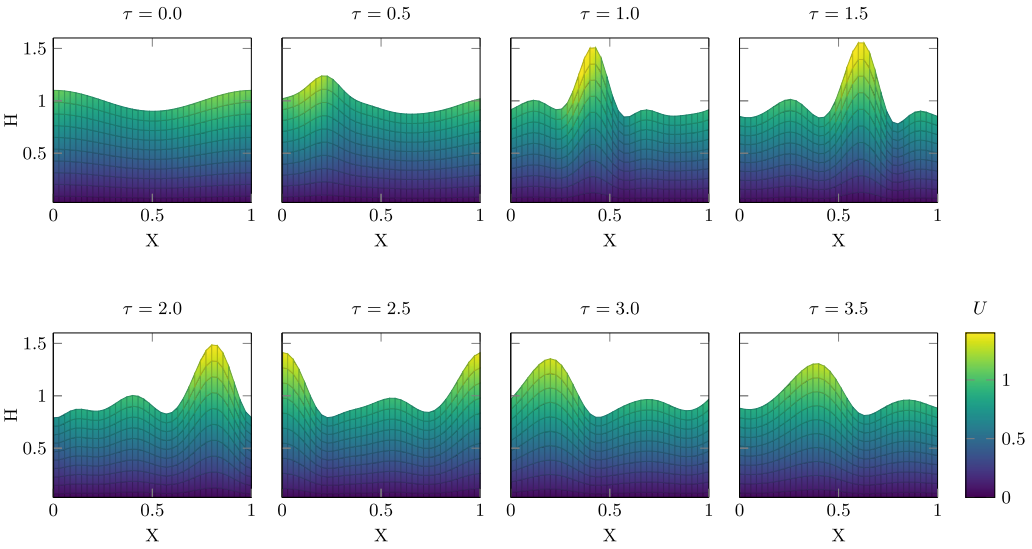

FIG. 5. Time evolution of the horizontal velocity field.

moderate reaction rate. The parameters are varied individually to determine their influence on the film development.

A. Influence of interfacial shear stress

The influence of the interfacial shear stress on the evolution of the maximum film height can be seen in Fig. 6. The behavior described in the preceding section can be observed. The maximum film

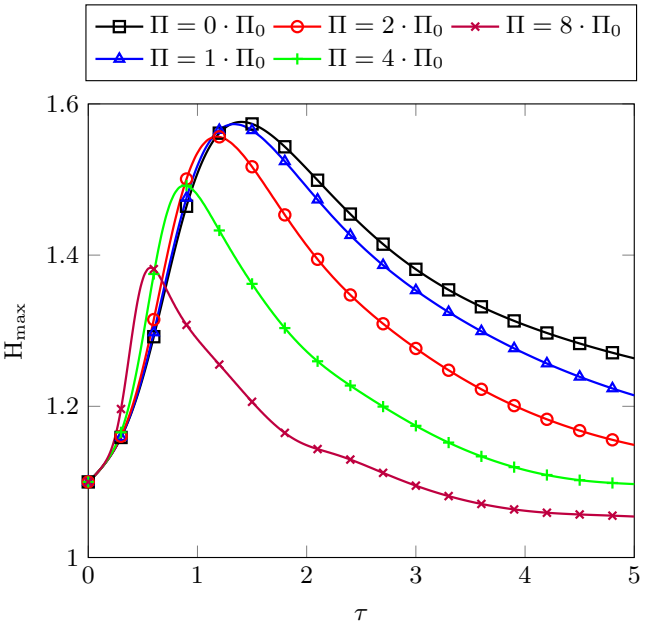

FIG. 6. Development of the film height maximum over time for varying interfacial shear stress.

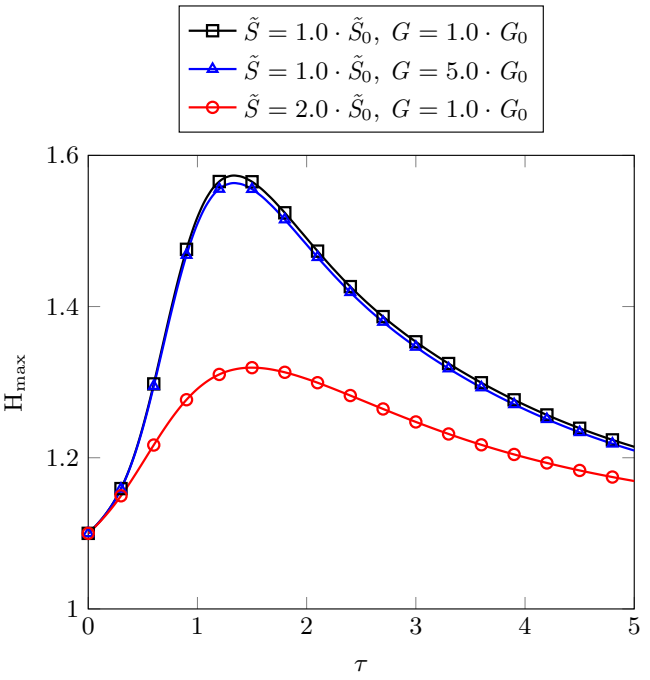

FIG. 7. Development of the film height maximum over time for varying surface tension force and gravity.

height increases with time until it reaches a peak value and then decreases asymptotically to the flat film height $H = 1$. From Fig. 6 one can conclude that the interfacial shear stress has a stabilizing effect on the film, since increasing shear stress leads to a reduced film height maximum. This result cannot be gained from the linear stability analysis in Sec. III and can only be found when solving the nonlinear evolution equation.

Furthermore, the film height maximum is reached at earlier time instances with increasing shear stress. In addition, the initial growth rate of the maximum film height is higher. This can be explained by looking at the horizontal velocity profile in Fig. 5. The velocity on the upstream side of the peak is higher than on the downstream side for small times, leading to the development of a narrow and high peak. This effect becomes stronger with increasing shear stress as the velocity magnitude increases.

Higher shear stress also leads to a quicker reduction of the maximum film height after the reaction has slowed down and the maximum disturbance is reached. With increasing shear stress, the peaks become narrower and the curvature higher. Thus, the surface tension force is larger in cases with high shear stress. This leads to to a faster decrease of the peaks after the influence of the reaction becomes negligible and the film evolution is dominated by surface tension.

B. Influence of surface tension and gravity

Figure 7 summarizes the surface tension and gravitational effect on the film evolution. As one can see, increasing the surface tension force leads to a more stable film, as has also been concluded from the linear stability analysis in Sec. III. In Fig. 7 a film with double the surface tension compared to the reference case shows a 48% decrease in the peak film height and also reaches the state of a flat film earlier after the reaction rate has decreased.

Gravity also has a stabilizing effect on the film, as is evident from Fig. 7. However, the effect is much weaker than that of surface tension. A five times higher gravitational force than in the reference case only leads to a decrease in maximum film height of about 5%. The initial film development is almost the same. Only with increasing time does the gravitational effect become more noticeable. It

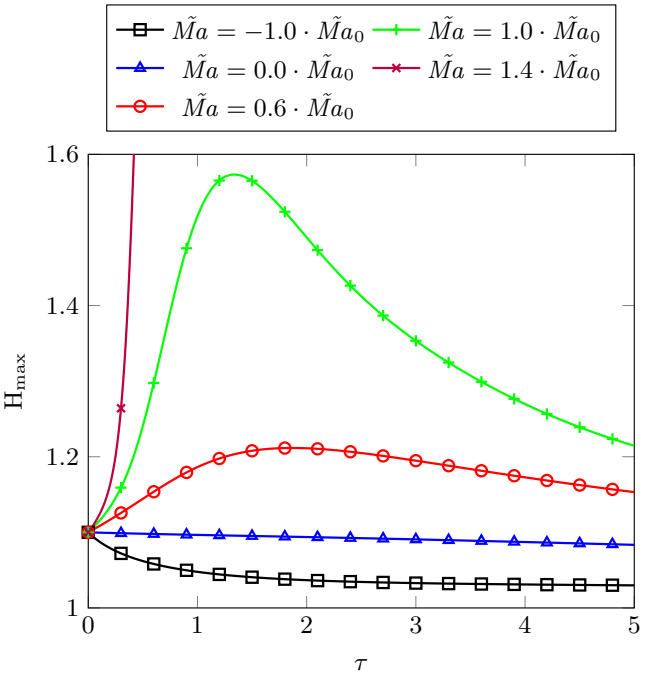

FIG. 8. Development of the film height maximum over time for varying reaction parameters.

can be concluded that the gravitational effect can be neglected when investigating thin shear stress driven oil films with chemical reactions in the chosen parametric setting. In this case the evolution equation can be reduced to

$$H_\tau + \frac{\epsilon}{\mathrm{Da}}\left[\frac{1}{2}\Pi H^2 + \epsilon\left(\frac{1}{3}\tilde{S}H^3 H_{XXX} - \frac{1}{2}\widetilde{\mathrm{Ma}}\, H_X H^3 e^{-\tau}\right)\right]_X = 0. \tag{42}$$

C. Influence of reaction parameters

It has been shown that an endothermic reaction has a destabilizing effect on the film, while an exothermic reaction is stabilizing as long as surface tension decreases with temperature. With increasing heat consumed by an endothermic reaction the maximum film height increases (Fig. 8). The film is very sensitive to the reaction parameters. An increase of the heat consumed by the reaction of 66% (from $0.6\,\widetilde{\mathrm{Ma}}_0$ to $1.0\,\widetilde{\mathrm{Ma}}_0$) leads to an increase of the peak film height of 190%. If the reaction is a little bit faster or consumes a little more heat than in the reference case, film rupture can be observed ($1.4\,\widetilde{\mathrm{Ma}}_0$). In the case of rupture the calculation is stopped since the derived model does not account for contact line phenomena.

Figure 8 also shows a film with no reaction ($\widetilde{\mathrm{Ma}} = 0$). In this case no growing film height maximum can be observed and surface tension and gravitational forces slowly lead to a flat film.

The stabilization is enhanced by an exothermic reaction ($-1.0\,\widetilde{\mathrm{Ma}}_0$) where the heat released by the reaction causes temperature maxima at the film crests and minima at the troughs. The resulting Marangoni effect leads to a convective flow from the crests to the troughs, and thus reduces film height maxima. The influence of the exothermic reaction on the stabilization of the film reduces with time as the reaction rate decreases, which can be seen in Fig. 8 when comparing the exothermic reaction to the film with no reaction.

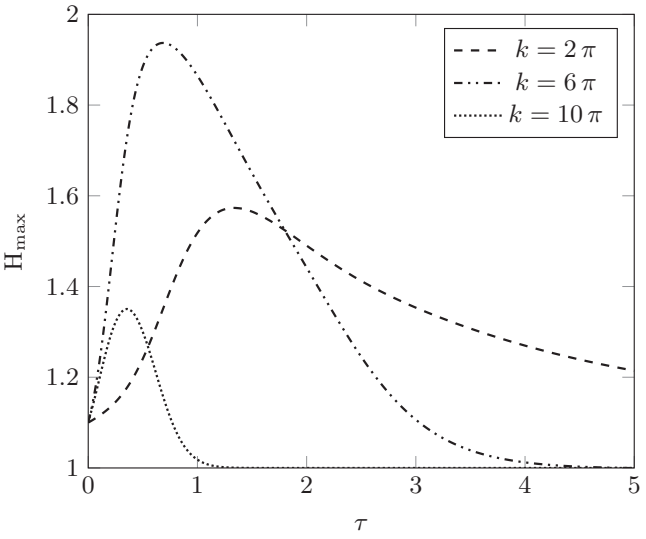

FIG. 9. Time evolution for different wave numbers of initial disturbance.

D. Influence of initial disturbance wavelength

Equation (34) shows the functional dependence of the growth rate on the wave number. Figure 2 shows the real part of the growth rate over the wave number for different times. For small times the growth rate increases from zero for small wave numbers, reaches a maximum value, decreases, and eventually becomes negative. With increasing time the maximum growth rate decreases and shifts to lower wave numbers. The three vertical lines in Fig. 2 correspond to films with three identical parameters but different initial disturbance wavelengths.

The evolution of the maximum film height over time for these three cases is shown in Fig. 9. In the low-wave-number case ($k = 2\pi$) the growth rates are low for all times (compare Fig. 2). This leads to a moderate increase in the maximum film height and also a moderate decrease after the reaction has slowed down at $\tau \approx 1.4$.

For a higher wave number of the initial disturbance ($k = 6\pi$) larger growth rates especially at lower times compared to the low-wave-number case are found (Fig. 2). This leads to a higher slope in the film height maximum. Additionally, a higher peak value is reached for $k = 6\pi$. For $\tau \approx 1.5$ the growth rate becomes negative for $k = 6\pi$ and the film height maxima decrease. This decrease is faster than for the film with the initial disturbance of low wave number (Fig. 9).

It can be shown that the highest crests in the film are observed for $k \approx 6\pi$ in this parameter setting. This is somewhat surprising since the growth rate at $\tau = 0$ has its maximum at $k \approx 9\pi$ (Fig. 2). However, the maximum growth rate shifts to lower wave numbers with increasing time and at $\tau \approx 0.6$ the maximal growth rate corresponds to $k = 6\pi$. Additionally, the disturbance growth rate stays positive for a longer period when the wave number is smaller. It should be noted that, due to nonlinear effects, it is not possible to predict the disturbance wavelength corresponding to highest peaks of film thickness or to film rupture from the laminar stability analysis.

If the wave number of the initial disturbance is increased even further ($k = 10\pi$), the initial increase rate in the maximum film height is similar to that in the case $k = 6\pi$ (Fig. 9). This can be explained from Fig. 2 with the similar growth rates of $\tau = 0$. However, the peak in the maximum film height is reached much earlier for $k = 10\pi$ ($\tau \approx 0.4$) and has a lower value. From there the maximum film height decreases rapidly and reaches a flat film shape for $\tau \approx 1.5$. In Fig. 2 this behavior correlates very well with the shown growth rates. For $\tau = 0.5$ the growth rate is already negative in this case and continues to drop rapidly with increasing time.

VI. CONCLUSION

A two-dimensional thin liquid film sheared by an outer gas flow has been investigated in which a chemical reaction takes place and leads to thermal Marangoni effects. The amount of reactant in the film is limited, so the reaction rate decreases with time. A long-wave evolution equation for the film thickness has been derived using a double perturbation analysis. A linear stability analysis has been performed. It has been found that surface tension and gravity stabilize the film. The chemical reaction is destabilizing for an endothermic reaction and stabilizing for an exothermic reaction, which is consistent with the results of previous studies (e.g., [16,17,26]).

Since the reaction rate is a decreasing function of time, the effect of the reaction on film stability and dynamics becomes weaker with time. For an endothermic reaction an initially unstable film can become stable with time. The reaction causes a growth of the initial disturbance to a maximum value before surface tension and gravity lead to the film flattening. For high reaction rates, however, the film ruptures before gravity and surface tension overcome the destabilizing effect of the chemical reaction.

The shear stress at the liquid-gas interface has a significant effect on the film evolution. With increasing shear stress, the growth rate of the disturbances is initially higher as the shear stress leads to higher and thinner film height maxima. With increasing time and decreasing reaction rate, however, surface tension decreases film height maxima. Due to the higher curvature of the peaks for higher interfacial shear stress, the surface tension force increases with increasing shear stress, which leads to faster film flattening. Overall, the interfacial shear stress was found to have a stabilizing effect on the film. This can only be found from solving the complete evolution equation and cannot be revealed from the linear stability analysis.

The wavelength of the initial disturbance has been found to have a crucial influence on the film evolution. The dependence of growth rate on wave number changes with time, so the critical initial disturbance has to be found iteratively.

In this work diffusive mass transport in the direction normal to the wall was neglected because the film is very thin. For future work it would be interesting to extend the evolution equation to include diffusive mass transport. In addition, solutocapillarity should be considered if the surface tension of the reactant and product species are significantly different. Higher-order convective terms could be included to get a more detailed look at the influence of those effects on the evolution of the film.

ACKNOWLEDGMENT

This work was supported by the German Research Foundation (DFG) under Collaborative Research Centre SFB/TRR150 Project No. B01.

[1] M. C. Drake, T. D. Fansler, A. S. Solomon, and G. A. Szekely, Jr., Piston fuel films as a source of smoke and hydrocarbon emissions from a wall-controlled spark-ignited direct-injection engine, SAE Report No. 2003-01-054, 2003 (unpublished).

[2] K. Schintzel, Kohlenwasserstoff-emissionen eines motors mit benzin-direkteinspritzung und wandgeführtem brennverfahren, Ph.D. thesis, Otto-von-Guericke-Universität Magdeburg, 2005.

[3] F. Zhao, M.-C. Lai, and D. L. Harrington, Automotive spark-ignited direct-injection gasoline engines, Prog. Energy Combust. Sci. **25**, 437 (1999).

[4] P. Dagaut, G. Pengloan, and A. Ristori, Oxidation, ignition and combustion of toluene: Experimental and detailed chemical kinetic modeling, Phys. Chem. Chem. Phys. **4**, 1846 (2002).

[5] B. S. Greensfelder, H. H. Voge, and G. M. Good, Catalytic and thermal cracking of pure hydrocarbons: Mechanisms of reaction, Ind. Eng. Chem. **41**, 2573 (1949).

[6] K. Norinaga and O. Deutschmann, Detailed kinetic modeling of gas-phase reactions in the chemical vapor deposition of carbon from light hydrocarbons, Ind. Eng. Chem. Res. **46**, 3547 (2007).
[7] L. Zhang, J. Cai, T. Zhang, and F. Qi, Kinetic modeling study of toluene pyrolysis at low pressure, Combust. Flame **157**, 1686 (2010).
[8] O. Güralp, P. Najt, and Zoran S. Filipi, Method for determining instantaneous temperature at the surface of combustion chamber deposits in an HCCI engine, J. Eng. Gas Turbines Power **135**, 081501 (2013).
[9] M. Kinoshita, A. Saito, M. Souchi, H. Shibata, and Y. Niwa, A method for suppressing formation of deposits on fuel injector for direct injection gasoline engine, SAE Report No. 1999-01-3656, 1999 (unpublished).
[10] W. Brack, Untersuchung der ablagerungsbildung durch harnstofffolgeprodukte im abgasstrang, Ph.D. thesis, Karlsruhe Institute of Technology, 2016.
[11] Z. Dagan and L. M. Pismen, Marangoni waves induced by a multistable chemical reaction on thin liquid films, J. Colloid Interface Sci. **99**, 215 (1984).
[12] F. K. von Gottberg, T. A. Hatton, and K. A. Smith, Surface instabilities due to interfacial chemical reaction, Ind. Eng. Chem. Res. **34**, 3368 (1995).
[13] Q. Qi and R. E. Johnson, Gravity-driven reactive and coating flow down an inclined plane, AIChE J. **40**, 2 (1994).
[14] R. J. Braun, B. T. Murray, W. J. Boettinger, and G. B. McFadden, Lubrication theory for reactive spreading of a thin drop, Phys. Fluids **7**, 1797 (1995).
[15] D. Gallez, A. De Wit, and M. Kaufman, Dynamics of a thin liquid film with a surface chemical reaction, J. Colloid Interface Sci. **180**, 524 (1996).
[16] P. M. J. Trevelyan, S. Kalliadasis, J. H. Merkin, and S. K. Scott, Dynamics of a vertically falling film in the presence of a first-order chemical reaction, Phys. Fluids **14**, 2402 (2002).
[17] P. M. J. Trevelyan and S. Kalliadasis, Dynamics of a reactive falling film at large Péclet numbers. I. Long-wave approximation, Phys. Fluids **16**, 3191 (2004).
[18] O. K. Matar and P. D. M. Spelt, Dynamics of thin free films with reaction-driven density and viscosity variations, Phys. Fluids **17**, 122102 (2005).
[19] A. Pereira, P. M. J. Trevelyan, U. Thiele, and S. Kalliadasis, Thin films in the presence of chemical reactions, Fluid Dyn. Mater. Proc. **3**, 303 (2007).
[20] R. V. Craster and O. K. Matar, Dynamics and stability of thin liquid films, Rev. Mod. Phys. **81**, 1131 (2009).
[21] A. Oron, S. H. Davis, and S. G. Bankoff, Long-scale evolution of thin liquid films, Rev. Mod. Phys. **69**, 931 (1997).
[22] R. Eötvös, Ueber den zusammenhang der oberflächenspannung der flüssigkeiten mit ihrem molecularvolumen, Ann. Phys. (Leipzig) **263**, 448 (1886).
[23] L. W. Schwartz, R. V. Roy, R. R. Eley, and S. Petrash, Dewetting patterns in a drying liquid film, J. Colloid Interface Sci. **234**, 363 (2001).
[24] P. H. Gaskell, P. K. Jimack, M. Sellier, and H. M. Thompson, Flow of evaporating, gravity-driven thin liquid films over topography, Phys. Fluids **18**, 013601 (2006).
[25] M. Schäfer, *Computational Engineering: Introduction to Numerical Methods* (Springer, Berlin, 2006).
[26] A. Pereira, P. M. J. Trevelyan, U. Thiele, and S. Kalliadasis, Interfacial instabilities driven by chemical reactions, Eur. Phys. J. Spec. Top. **166**, 121 (2009).